Transient Ordered Domains in Single-Component Phospholipid Bilayers

Teemu Murtola,[1] Tomasz Róg,[2,3] Emma Falck,[4] Mikko Karttunen,[5] and Ilpo Vattulainen[1,6,7]

[1]*Laboratory of Physics and Helsinki Institute of Physics, Helsinki University of Technology, FI-02015 Espoo, Finland*
[2]*Biophysics and Statistical Mechanics Group, Laboratory of Computational Engineering, Helsinki University of Technology, FI-02015, Finland*
[3]*Department of Biophysics, Faculty of Biotechnology, Jagellonian University, PL-30387 Krakow, Poland*
[4]*Beckman Institute for Advanced Science and Technology, University of Illinois at Urbana-Champaign, Illinois 61801, USA*
[5]*Department of Applied Mathematics, The University of Western Ontario, London, ON, Canada N6A 5B7*
[6]*Institute of Physics, Tampere University of Technology, FI-33101 Tampere, Finland*
[7]*Memphys-Center for Biomembrane Physics, Physics Department, University of Southern Denmark, DK-5230 Odense M, Denmark*

(Received 29 June 2006; published 7 December 2006)

We report evidence of dense, ordered nanodomains in single-component fluid lipid bilayers. Our atomic-scale molecular dynamics simulations suggest that the area available to a lipid acyl chain exhibits large fluctuations, resulting in denser and sparser domains. The sizes of the dense domains can be up to $\sim$10 nm, and their lifetimes are of the order of $\sim$10 ns. In addition, our simulations suggest that domains of lipids with highly ordered acyl chains form predominantly within the dense regions, their sizes ranging from a few chains up to a few nanometers, and with lifetimes between $\sim$10 ps–10 ns. These observations shed light on the origin of experimentally observed fluctuations, as well as on the mechanisms of phase transitions in lipid membranes.

DOI: 10.1103/PhysRevLett.97.238102 PACS numbers: 87.14.Cc, 02.70.Ns, 87.16.Dg

Biological membranes form an environment for a variety of biomolecular assemblies and biochemical processes. The possible existence of nanoscale domains in biological membranes, the so-called lipid raft hypothesis [1], has been the subject of enormous attention. Of particular interest is their phase behavior, which is poorly understood. Consequently, a variety of studies have focused on model ternary mixtures containing cholesterol, and saturated and unsaturated lipids, but the phase behavior of these systems is not well understood either [2–4]. Even more puzzling is the fact that there is still some doubt about the nature of the coexistence region in binary mixtures containing cholesterol. In fact, even the phase behavior of single-component bilayers is not fully understood [5,6].

Many experimental and theoretical studies have shown that single-component phospholipid bilayers exhibit critical-like spatial fluctuations when the main transition temperature T_M is approached from the fluid (L_α) phase [6–9]. Also other properties, such as the lamellar spacing in multilamellar vesicles, show critical-like behavior in this region [10]. The main transition also has features of first-order transitions. Several explanations have been proposed, such as the transition being only weakly first order [7,11], or the occurrence of small gel-like domains within the fluid phase [6]. However, direct observation of the microscopic features is experimentally very difficult, and the details of the behavior have remained elusive.

In this Letter, we employ atomistic molecular dynamics (MD) simulations to study the critical-like fluctuations. We demonstrate the presence of transient highly ordered domains in the L_α phase close to T_M. We also see longer-lived domains of high density. These nanodomains are characterized in detail. The observations shed light on the microscopic origin of the critical fluctuations and the mechanism(s) of phase transitions in lipid membranes.

We performed a 40 ns simulation of a lipid bilayer consisting of 1152 fully hydrated dipalmitoylphosphatidylcholine (DPPC) molecules, modeled using a thoroughly validated DPPC force field [12–14]. The electrostatics were treated with the reaction field method; no qualitative differences were observed with a 10 ns simulation with particle-mesh Ewald electrostatics. The simulations were performed in the NpT ensemble, with the $T = 323$ K (above $T_M \approx 315$ K). The first 10 ns was treated as equilibration, since after 10 ns, the area per lipid had clearly stabilized; i.e., the lipids had had enough time to diffuse from their initial positions (see Ref. [15]). All simulations were carried out using GROMACS [16]. Other details can be found in the supplementary material [15].

Figures 1(a)–1(d) show selected visualizations summarizing our results. All snapshots are from the same configuration, chosen near the end of the trajectory. Figure 1(a) shows the area available to each lipid chain in one monolayer. The areas have been calculated using a 2D Voronoi tessellation [17] of the the center-of-mass (c.m.) positions of the acyl chains. While undulations are not accounted for in this analysis, we found that the effects seen in the figure are practically uncorrelated with the undulations (see below).

Figure 1(a) shows that there are clearly domains of higher and lower densities. However, there is also a substantial variation in the area available within these domains, and the domain borders are not sharp. Visual inspection of the dynamics of the system [15] shows that

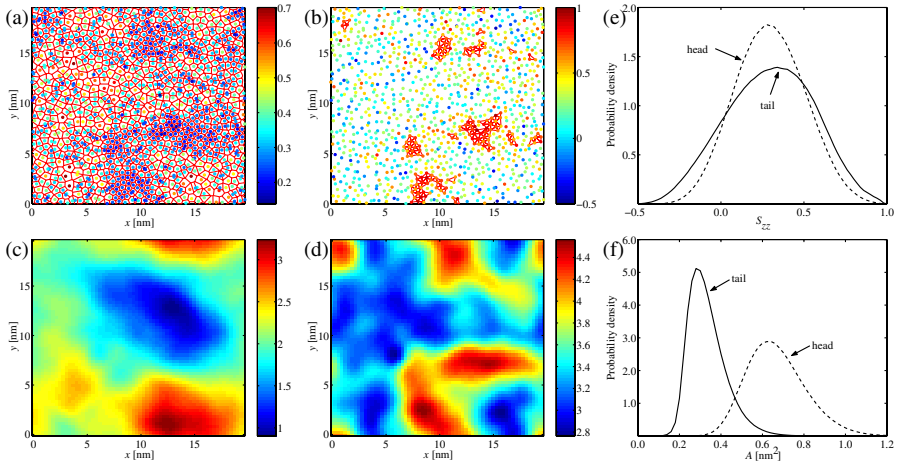

FIG. 1 (color online). Visualization of a single configuration of 1152 molecule lipid bilayer together with probability distributions of order parameter and area per chain or head group. Panel (a) shows the area per tail in one monolayer, determined using a Voronoi tessellation of the c.m. coordinates of the tails. Panel (b) shows the average order parameter S_{zz} for each tail in the same configuration; the extremum values of S_{zz} are 1 and -0.5, corresponding to a perfectly ordered (all-trans) state and a conformation perpendicular to the membrane normal, respectively. Lack of order is characterized by $S_{zz} \approx 0$. Panels (c) and (d) show the undulations and the membrane thickness, respectively. Panels (e) and (f) show the probability distributions of the order parameters and the areas for the whole trajectory. The head group order parameter was defined as the average of the chain order parameters.

the denser domains have long lifetimes, with the density staying largely unaltered over a period of at least 10 ns. A similar figure for the other monolayer (not shown) indicates that the locations of the denser regions are significantly correlated across the bilayer. This observation is in line with the recent work of Marrink *et al.* on the dynamics of the main transition using a coarse-grained model [18]. They observed that gel domains formed preferentially at the same locations in the opposite monolayers.

Large differences in packing suggest different ordering in different regions. This is indeed true: Fig. 1(b) shows the average order parameter for each chain. It is given by $S_{zz} = \frac{1}{2}\langle 3\cos^2\theta_i - 1\rangle_i$, where θ_i is the angle between the bilayer normal (lying along the z direction) and the molecular axis which connects the neighboring carbon atoms $i-1$ and $i+1$, and $\langle\cdot\rangle_i$ denotes an average over all the carbon atoms in the chain.

Figure 1(b) clearly shows some larger clusters of high ordering, but there is also significant local variation. To visualize the clusters, we denote a chain as ordered if $S_{zz} > 0.5$ and it has at least two neighboring chains (defined by Voronoi tessellation) satisfying the same criterion. The figure shows that there are small ordered clusters (consisting of a few chains) in addition to the larger ones. These clusters are located predominantly in the denser regions. Contrary to the dense domains, these clusters are highly dynamic [15], and their shape can change significantly over a period of a few hundred picoseconds. Despite these temporal fluctuations in shape, the larger clusters have lifetimes of the order of nanoseconds. The smaller clusters, on the other hand, form and disappear on the time scales of tens or hundreds of picoseconds. The conclusions are similar for other threshold values besides 0.5.

We also compared the locations of the domains to the undulations and thickness of the membrane. These quantities were calculated on a grid using smooth interpolation with a Gaussian kernel and 1 nm bandwidth. First, the head group c.m.s were used to calculate the z coordinate for both monolayers. The average and difference of these coordinates were then used to describe the undulations and the thickness, respectively. The results are shown in Figs. 1(c) and 1(d). Comparison with the other snapshots shows no apparent correlation between the density or order and the undulations. However, the density correlates strongly with the thickness, as the total volume cannot vary as strongly as the area.

Distributions for the areas and the order parameters are shown in Figs. 1(e) and 1(f). All distributions are smooth and single peaked, and the tail ones have a slight asymmetric tail towards more disordered regions (larger areas). Hence, there is no clear division between ordered and disordered, or dense and sparse regions. This also shows that the fluctuations in the system are very strong, obscuring any possible difference in the probability distributions of the different domains. The distributions for S_{zz}^{head} and A_h can be fitted well with normal and log-normal distributions, respectively. For S_{zz}^{tail} and A_t there are larger systematic deviations, but the same distributions give the best fit.

It is logical to ask whether also the area per head group is smaller in denser and/or more ordered regions. The connection is much weaker here (figure not shown): the area per head group may be slightly smaller in the denser regions, but the effect is obscured by large fluctuations, see Fig. 1(f). It is possible that the larger size of the head group prevents the formation of larger dense clusters: although the chains can pack easily to form tight

clusters, the head groups are more bulky and cannot pack as closely.

To quantitatively assess the validity of the above inference about the correlations, we calculated correlation coefficients c_{ab} between different quantities a and b. The maximum and minimum values of c_{ab} are 1 and -1, respectively, corresponding to a perfect linear relationship with a positive or a negative coefficient. A value close to zero indicates that there is no apparent linear relationship. Quantities in the same monolayer were compared for each particle, and for comparisons between different monolayers (and with properties of the whole bilayer) we used a smooth kernel averaging as described earlier. For details of the correlation coefficients, see Ref. [15].

Table I shows the correlation coefficients for the local order parameter S_{zz}, the area per chain A_t and per head group A_h, and the thickness of the membrane d and the z coordinate of the membrane. The upper left corner confirms that A_t and S_{zz} are correlated: the correlation coefficient is -0.32, and increases to -0.46 for kernel-averaged quantities. In contrast, A_h has a much weaker correlation with both S_{zz} and A_t, showing that the head group packing is not as strongly connected to ordering. However, some correlations emerge for the kernel-averaged quantities. The upper right corner shows that the transmembrane correlations are the strongest for A_t, with only minor correlations observed for the other quantities.

For the undulations (represented by z), the correlation coefficients vary between 0.1 and 0.3 and are asymmetric over the monolayers. Thus there may be some effects from the undulations, but they are not the main cause of the observed phenomena. The asymmetry between the monolayers may be associated with asymmetric undulations. In contrast, the correlation between d and A_t is very strong, in agreement with the volume argument above. Yet again, the correlation of d with A_h is weaker.

The calculated correlation coefficients support all the conclusions drawn from Fig. 1. However, the values are typically below 0.5. This indicates either that the relationship between the quantities is not linear, and/or that there are strong, independent fluctuations in all quantities. Figure 2 shows the bivariate distribution for A_t and S_{zz}. The distributions for other pairs are similar, demonstrating that fluctuations are the main reason for the low values.

TABLE I. Intra- and intermonolayer correlation coefficients between local order parameter S_{zz}, area per chain A_t, area per head group A_h, membrane thickness d, and membrane z coordinate. Transmembrane comparison (last three columns), and comparison involving d and z, were done using smooth kernel averaging (see text) for all quantities. Also intramonolayer correlation coefficients for the kernel-averaged quantities are given (middle three columns).

				Kernel-averaged					
	Same monolayer			Same monolayer			Other monolayer		
	S_{zz}	A_t	A_h	S_{zz}	A_t	A_h	S_{zz}	A_t	A_h
S_{zz}		-0.32	-0.11		-0.46	-0.20	0.10	-0.21	-0.18
A_t			0.15			0.38		0.48	0.33
A_h									0.22
d				0.42	-0.82	-0.44			
z				-0.31	0.08	-0.05	0.05	-0.29	0.17

We further elucidated the nature of the domains. First, we calculated the static structure factors $S(k)$ for the monolayers after projecting the c.m. coordinates to the x-y plane. The static structure factor is defined by $S(k) = \langle \rho(k)\rho(-k)\rangle/N$, where $\rho(k)$ is the Fourier transform of the particle density and N is the total number of particles. The expression for $S(k)$ can be separated into contributions from different pairs of particles by using the densities of specific particle types in the expression.

The static structure factors for different pairs are shown in Fig. 3. There is a clear peak at small k, coming mostly from the chain-chain structure factor. This is in line with the presence of large spatial density fluctuations, and also shows that there is no clear length scale for the denser regions, apart from the system size. Structure factors calculated over different parts of the trajectory (not shown) demonstrate that these domains develop very slowly. In fact, the peaks are still growing after 20 ns. Hence, the domains are not a consequence of poor equilibration, but care should be taken when interpreting the quantitative results. The presence of the domains in equilibrium is also supported by large-scale simulations of a coarse-grained model, constructed based on a smaller MD system using the Inverse Monte Carlo technique [19].

We also calculated the size distribution of the ordered clusters shown as an inset in Fig. 3. It is monotonically decreasing, with the majority of the clusters being formed by just a few chains. Thus, there is no dominant size.

The dynamics of the ordered clusters turned out to be complex. The clusters may easily split up and merge with others, which makes defining a lifetime for a cluster difficult. Following the largest fragment of each cluster until it completely disappears, we get lifetimes of tens of picoseconds for the smallest clusters and a few nanoseconds for the largest ones. In contrast, calculating transition probabilities between different sized clusters, again based on the largest fragments, we get expected lifetimes of a few hundred picoseconds for the largest clusters. The fact

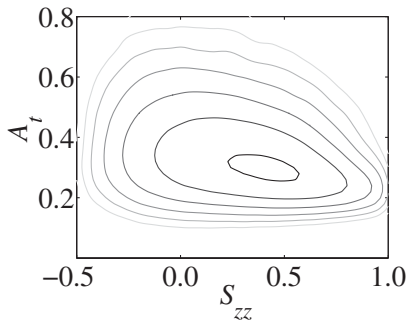

FIG. 2. Bivariate probability distribution of area per tail A_t and order parameter S_{zz}. The contours are on logarithmic scale.

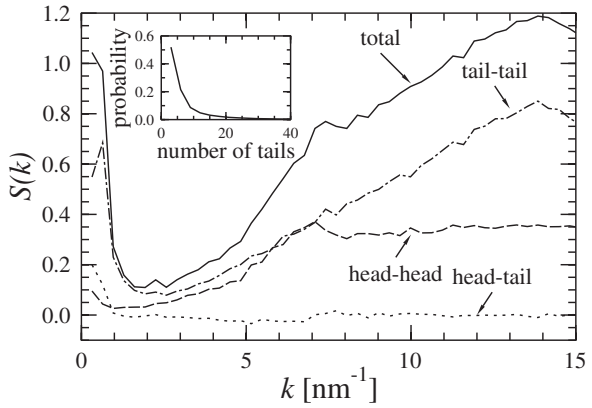

FIG. 3. Static structure factors calculated for 2D center-of-mass coordinates and averaged over monolayers. The inset shows the size distribution of ordered domains. The size was measured as the number of ordered chains ($S_{zz} > 0.5$).

that the latter estimate is too small indicates that the chains cannot be easily classified as just ordered or disordered. Instead, chains that become ''disordered'' are likely to be part of a reconstructed cluster after some time.

Let us finally briefly discuss the relevance of our results. The reported simulations provide atomic-scale insight into the nature of the density fluctuations, information which cannot be easily accessed experimentally or with simple theoretical models. For example, our results indicate that the increase in the bilayer thickness observed by Zhang *et al.* [10] is not uniform, but occurs predominantly in the denser regions. In general, our results agree at least qualitatively with other studies of the critical behavior. However, they also reveal the complexity of the phenomenon, since the properties of the domains are very different for the density and the local order. It is also likely that other local properties, such as the lateral pressure profile, are different in different parts of the membrane. Such inhomogeneity could facilitate changes in the membrane protein conformational states and hence affect the functioning of membrane proteins. While studies of temperature dependence were beyond our reach in this work, further simulations at different temperatures could prove useful to characterize the critical behavior close to T_M.

The present results indicate the formation of transient domains even in single-component lipid bilayers when the system is relatively close to T_M. This suggests that similar domains could also occur in more complex systems. At the simplest level, it is possible that ordered domains could exhibit interesting interplay with cholesterol in binary and ternary mixtures. The present results provide a starting point and motivation for such studies.

In conclusion, we have studied fluctuations in the local density and order parameters of a single-component lipid bilayer using atomistic MD simulations. The results show clear domains of higher and lower densities with long characteristic times. The domains are correlated across the bilayer. The denser areas show transient domains of high ordering, with the largest domains consisting of up to 50 lipids. For both quantities the temporal fluctuations are strong, obscuring any possible presence of two different phases and making the domain boundaries difficult to define. The presented results agree with experiments, and give insight into the atomistic origin of the phenomenon.

We acknowledge support by the Academy of Finland, the National Graduate School in Nanoscience, Marie Curie Intra-European Grant No. 024612-Glychol, the Beckman Institute, the National Science and Engineering Research Council of Canada, and the Emil Aaltonen Foundation.

[1] K. Simons and E. Ikonen, Nature (London) **387**, 569 (1997).
[2] S. L. Veatch and S. L. Keller, Phys. Rev. Lett. **89**, 268101 (2002).
[3] S. L. Veatch and S. L. Keller, Phys. Rev. Lett. **94**, 148101 (2005).
[4] R. Elliott, I. Szleifer, and M. Schick, Phys. Rev. Lett. **96**, 098101 (2006).
[5] G. Pabst, H. Amenitsch, D. P. Kharakoz, P. Laggner, and M. Rappolt, Phys. Rev. E **70**, 021908 (2004).
[6] D. P. Kharakoz and E. A. Shlyapnikova, J. Phys. Chem. B **104**, 10 368 (2000).
[7] S. Doniach, J. Chem. Phys. **68**, 4912 (1978).
[8] L. K. Nielsen, T. Bjørnholm, and O. G. Mouritsen, Nature (London) **404**, 352 (2000).
[9] L. K. Nielsen, A. Vishnyakov, K. Jørgensen, T. Bjørnholm, and O. G. Mouritsen, J. Phys. Condens. Matter **12**, A309 (2000).
[10] R. Zhang, W. Sun, S. Tristam-Nagle, R. L. Headrick, R. M. Suter, and J. F. Nagle, Phys. Rev. Lett. **74**, 2832 (1995).
[11] O. G. Mouritsen, Chem. Phys. Lipids **57**, 179 (1991).
[12] D. P. Tieleman and H. J. C. Berendsen, J. Chem. Phys. **105**, 4871 (1996).
[13] E. Falck, M. Patra, M. Karttunen, M. T. Hyvönen, and I. Vattulainen, Biophys. J. **87**, 1076 (2004).
[14] S. Vainio, M. Jansen, M. Koivusalo, T. Róg, M. Karttunen, I. Vattulainen, and E. Ikonen, J. Biol. Chem. **281**, 348 (2005).
[15] See EPAPS Document No. E-PRLTAO-97-081648 for technical details of the simulations, and some additional information about the correlation coefficients. There are two animations of dynamics in the system: one for average order parameters and another for areas per tail. There is also a figure showing the evolution of the area per lipid as a function of time. For more information on EPAPS, see http://www.aip.org/pubservs/epaps.html.
[16] E. Lindahl, B. Hess, and D. van der Spoel, J. Mol. Model. **7**, 306 (2001).
[17] W. Shinoda and S. Okazaki, J. Chem. Phys. **109**, 1517 (1998).
[18] S. J. Marrink, J. Risselada, and A. E. Mark, Chem. Phys. Lipids **135**, 223 (2005).
[19] T. Murtola, E. Falck, M. Karttunen, and I. Vattulainen (to be published).